Precision Engineering 44 (2016) 13–28

Contents lists available at ScienceDirect

Precision Engineering

journal homepage: www.elsevier.com/locate/precision

Review

Laser trackers for large-scale dimensional metrology: A review

Bala Muralikrishnan*, Steve Phillips, Daniel Sawyer

Engineering Physics Division, National Institute of Standards and Technology, Gaithersburg, MD 20899, United States

ARTICLE INFO

Article history:
Received 11 September 2015
Received in revised form
30 November 2015
Accepted 2 December 2015
Available online 21 December 2015

Keywords:
Laser tracker
Large-scale dimensional metrology
Error modeling
Performance evaluation
Measurement uncertainty
Standardization

ABSTRACT

Thirty years since their invention, laser trackers are now recognized as the measurement tool of choice in the manufacture and assembly of large components. The general design of laser trackers, i.e., a ranging unit on a two-axis gimbal, has not changed significantly over the years. However, innovations in ranging technology, for example, the emergence of increasingly accurate absolute distance meters (ADMs), are providing users with an alternative to interferometers (IFMs). Hand-held accessories such as touch probes and line scanners are expanding the scope and applicability of laser trackers. In this paper, we survey the literature in all areas of laser trackers as applied to large-scale dimensional metrology (LSDM), with emphasis on error modeling, measurement uncertainty, performance evaluation and standardization.

Published by Elsevier Inc.

Contents

* Corresponding author. Tel.: +1 301 975 3789.
E-mail address: balam@nist.gov (B. Muralikrishnan).

http://dx.doi.org/10.1016/j.precisioneng.2015.12.001
0141-6359/Published by Elsevier Inc.

1. Introduction

The laser tracker was invented in the mid-1980s by Lau et al. [1–3] at the National Institute of Standards and Technology (NIST) to facilitate robot metrology. Laser trackers are portable coordinate measuring systems (CMS) that measure the three-dimensional coordinate position of a cooperative target such as a spherically mounted retroreflector (SMR). The instrument records the distance to the target along with two angles, providing position data in a spherical coordinate system. Two closely related spherical coordinate systems are a coherent laser radar based system [4] and the laser tracer [5]. The coherent laser radar based system operates without the need for a cooperative target and does not track the target. In that sense, it is more closely related to large volume terrestrial laser scanners and therefore not considered in this review. The laser tracer does require a cooperative target and tracks the target in the same manner a tracker does. The laser tracer, however, only reports range to the target and not angles, and is intended to be used in a multilateration scheme (see Section 3.3).

Much of the research and development activity during the last 30 years has been in the areas of absolute distance meter design, modeling of instrument error sources and estimation of uncertainty, improving accuracy using multilateration, design and testing of hand held accessories, and the development of performance evaluation methods and standardization. These efforts have tremendously increased the scope and applicability of laser trackers. Today, laser trackers are the measurement tool of choice for a multitude of applications (see Section 5). These include robot metrology, manufacture and assembly of large components such as aircraft wings and ship hulls, error mapping of coordinate measuring machines (CMM) and machine tools, providing reference measurements for large volume laser scanners and distributed metrology systems (such as indoor GPS), automotive panel assembly using hand held accessories, and alignment of large optics and structures for astronomy and nuclear industry. In this paper, we survey reported literature in all research areas of laser trackers as applied to large-scale dimensional metrology (LSDM), with emphasis on error modeling, measurement uncertainty, performance evaluation and standardization.

This paper is organized as follows. The principles of laser tracker operation and the major sources of error are described in Section 2. This section includes discussions on ranging technology, opto-mechanical errors, geometrical error models, compensation procedures, targets, and hand-held accessories. In Section 3, we address improvements to measurement accuracy through multi-station measurements such as bundle-adjustment procedures and multilateration. Performance evaluation tests, documentary and material standards, traceability, and measurement uncertainty are covered in Section 4. We provide an overview of some of the applications in Section 5, followed by conclusions in Section 6.

2. Principles of operation and error sources

A laser tracker is comprised of several key sub-systems: the ranging unit, the two-axis steering mechanism, the tracking mechanism, environmental sensors, and targets. We describe the sub-systems, associated error sources, geometrical error models, and compensation procedures in this section.

2.1. Sub-systems

A laser tracker is an assembly of various mechanical and optical components. A schematic of one design of a tracker is shown in Fig. 1. The instrument has two rotation axes – a standing axis (vertical axis) and a transit axis (horizontal axis). In ideal geometrical configuration, the two axes are orthogonal to each other and intersect at a point that serves as the origin for the spherical coordinate system defined by the tracker. The path of the laser beam from the instrument to the target ideally intersects this origin and is perpendicular to the transit axis. One angle encoder is mounted coaxially with the standing axis to read the horizontal angle while the second encoder is mounted coaxially with the transit axis to read the vertical angle. The encoders are not shown in Fig. 1.

A portion of the beam emerging from the source (laser-head) is retained within the system as the reference beam for interferometric fringe counting. The measurement portion of the beam

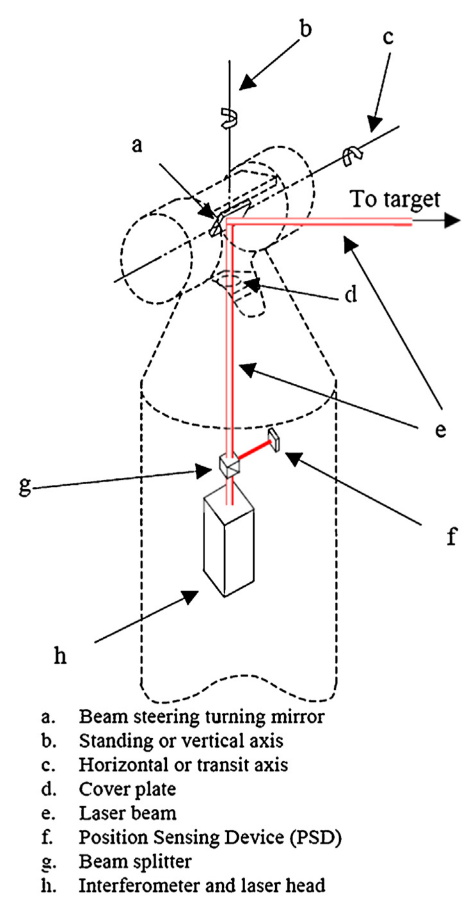

Fig. 1. Construction of a laser tracker with a beam steering mirror (angle encoders are not shown in the figure) [*Source*: Sawyer et al. [10], reproduced with permission from ASPE].

is reflected off the steering (tracking) mirror, strikes the retroreflector and returns to the tracker. A portion of the return beam is deflected to a position sensitive detector (PSD), while the remaining portion is directed to the fringe counter for range evaluation. Any radial movement of the SMR is detected by the range finder. Lateral movement of the SMR results in an offset of the spot on the PSD. The control system then exercises the two rotational axes of the instrument to re-center the spot on the PSD, thus continually tracking the target and hence providing real time angular coordinates of the target.

While Fig. 1 shows the schematic of a tracker that uses a beam steering mirror to direct the laser to the target, other designs of laser trackers are also available. Some manufacturers produce trackers that have the source in the base but emit the laser from the head through a fiber optic cable, while other manufacturers place the laser source itself in the head. The beam steering mirror is no longer necessary in each of these cases. An overview of the technology and some applications can be found in Refs. [6–9].

2.2. Ranging technology

Early versions of laser trackers, and even many manufactured today, are equipped with a He-Ne laser interferometer (IFM) for measuring radial displacement. The laser beam is split into two parts with one portion remaining within the instrument to act as the reference. The other part, known as the measurement beam, is steered to the target and is reflected back to the instrument. The measurement beam is superimposed on the reference beam, resulting in optical interference. This interference consists of bright and dark fringes, corresponding to constructive and destructive interference, respectively, between the two superimposed beams; a photodetector then converts the intensity into an electrical signal. As the path traversed by the measurement beam changes by a distance corresponding to half of its wavelength ($\lambda/2$), the optical interference alternates between bright and dark fringes. Thus, by counting the number of times the fringes are alternated (and by knowing λ), the displacement of the target can be calculated. IFMs can only measure relative displacement. In order to determine the absolute distance of the target from the center of rotation of the instrument (the origin for the spherical coordinate system), manufacturers provide a reference point on the body of the instrument, i.e., a home position, that is located at a known distance from the origin.

The accuracy of interferometric length measurements largely depends on the accuracy with which the wavelength of light can be determined in the measurement environment. It is well known that temperature, pressure, relative humidity, and composition of the air, affect refractive index [11–14] and, therefore, the wavelength of light in air. The ability of the environmental sensors to monitor and compensate for these parameters is critical to achieving high accuracies. At NIST, we currently achieve an expanded uncertainty ($k = 2$) of $1\ \mu\text{m} + 0.24 \times 10^{-6} L$ (where L is in units of meters) on reference length measurements up to 60 m using an interferometer in our tape tunnel facility [15]; the length dependent term is due to uncertainty associated with the refractive index and the constant term is associated with the mechanical setup of the optics. Among the parameters that affect refractive index, temperature is the most critical, contributing a relative displacement error of about 1 ppm/°C. We discuss environmental influence on laser tracker measurements in Section 4.6. The accuracy of an IFM based length measurement on a laser tracker not only depends on the environmental conditions but also on the stability of the home position. Manufacturers typically specify a maximum permissible error for this parameter, denoted $R0$ (zero-length or the home position) along with an $A + B \times L$ (constant and length dependent) type specification for the IFM errors.

An advantage of He-Ne IFMs is the robustness of the system, e.g., once the vacuum wavelength is metrologically verified it has long term stability (on the order 1×10^{-7}) [16]. Additionally, it has an inherently short metrological traceability path since it is one of the recommended radiations for the realization of the meter [17]. A disadvantage of IFM based trackers is the need to re-establish the home position of the target in the event of a break in the beam; this is because IFMs count the alternating light–dark fringes on the photodetector as the SMR is displaced and this count is lost if the beam breaks. Because there are many measurement tasks where it is a challenge to complete measurements without a break in the beam, tracker manufacturers began introducing absolute distance meters (ADMs) in addition to IFMs in their systems.

ADM systems typically determine distance to target by modulating the amplitude, frequency, or polarization of a laser beam and resolve distance to the target by phase measurements. Modulation techniques for measuring distance were first realized by Froome and Bradsell [18] in 1961. Thiel et al. [19] used continuous frequency modulation (chirping) to achieve ADM ranging up to 40 m with a relative uncertainty of 10^{-6}. Payne et al. [20] describe an amplitude modulated ADM with an accuracy of 50 μm for distances up to 120 m. Stone et al. [21] constructed a frequency modulated ADM and provide a detailed analysis of the uncertainty sources.

Conceptually, an ADM can be constructed by sinusoidally modulating the amplitude of a laser diode beam at a precise frequency. By comparing the phase of the return beam with a portion of the beam emerging from the laser diode, the location of the retroreflector within one modulated wavelength – known as the fringe fraction [22] – can be determined very accurately. (Note that one wavelength of phase shift corresponds to one-half wavelength of retroreflector displacement because the light is making a round trip from the reflector.) Unfortunately, there are usually many multiples of the modulated wavelengths between the laser and the reflector. This "ambiguity interval" is commonly resolved either by including additional modulation wavelengths or by continuously varying the frequency of modulation.

The cumulative phase shift between the measurement and reference arms of the interferometer is $4\pi nL/\lambda$ where n is the refractive index and L is the distance to the retroreflector minus the reference arm length and the factor of 4π (instead of 2π) is due to the round trip of the light. We allow this cumulative phase shift to take values much larger than 2π but recognize that we cannot distinguish between repeating intervals of 2π. If another measurement with a different modulation frequency is made and we examine the difference in the two cumulative phases, $4\pi nL(1/\lambda_1 - 1/\lambda_2) = 4\pi nL(\lambda_2 - \lambda_1)/\lambda_1\lambda_2 = 4\pi nL/\Lambda$ where $\Lambda = \lambda_1\lambda_2/(\lambda_2 - \lambda_1)$. Recalling that the observed fringe fraction for each wavelength is modulo 2π, let L_0 be the value of L where the two fringe fractions repeat. This requires the variable $m = 2\,n\,L_0/\lambda_1$ to be an integer and similarly requires $m\,(\lambda_2 - \lambda_1) = \lambda_2$ due to the repeat requirement. Hence, $(2\,n\,L_0/\lambda_1)\,(\lambda_2 - \lambda_1) = \lambda_2$ yielding $n\,L_0 = \Lambda/2$. The synthetic wavelength Λ is thus twice the optical path length of the ambiguity interval of the two frequency measurements; this synthetic wavelength can be made very large by choosing the two frequencies to be close to each other. If the two frequencies are on the order of 3 GHz and differ by 3 MHz then Λ is 100 m and one-half this amount determines the maximum range of the ADM. Phase discrimination of the fringe fractions of around 10^{-3} determines the particular ambiguity interval of a single modulated frequency and then the fringe fraction of that frequency is used to obtain a more finely resolved distance measurement. This method is capable of achieving accuracies comparable to that of IFMs in typical measuring environments. Since 2010, at NIST we have evaluated the ranging capability of several commercial ADM trackers at standard conditions (20 °C) and observed relative errors less than 5×10^{-7} over a distance of 3 m to 60 m.

There are many implementations of ADM technology addressing measurement ranges from short distances (<1 m) to very large distances (>100 m). Presently, for laser tracker applications, ADM relative accuracy of $\leq 10^{-6}$ on static targets is sufficient enough so it is not a binding accuracy constraint on the overall system; subsequently, other factors such as robustness, miniaturization, and cost become driving parameters.

2.3. Opto-mechanical errors

A number of geometrical and optical misalignments are possible in a practical realization of a laser tracker. These misalignments contribute to systematic errors in the measured range and angles. For example, non-orthogonality and non-intersection are error sources associated with the axes. There could exist an offset in the scale of the vertical angle encoder, that is, the zero does not coincide with the instrument's pole. Eccentricity of the rotational axes and angle-dependent scale errors are error sources associated with the encoders. A misaligned laser source produces a beam path that could be tilted and offset from the ideal path. If the tracker has a beam steering mirror, it is possible that the plane of the mirror does not contain the origin. The mirror itself may possibly be tilted in such a way as to direct the beam in a path other than the one intended. Incorrect calibration and drift of the $R0$ length are also errors. The vacuum as well as compensated wavelength of the interferometer could be incorrectly calibrated. The ADM may also have uncharacterized error sources and time-dependent drifts, each contributing to errors in range measurement. Any of the sources of error described here and other such sources results in systematic errors in the measured range and angles.

Given the similarity in construction between laser trackers and theodolites, some sources of error are common to both instruments. As a result, modeling of errors in laser trackers benefited from extensive past work on theodolite and total station error analysis literature. We do not survey theodolite or total station literature here; we refer to Deumlich [23] for an overview of theodolite error sources and models.

Lau et al. [3] describe early work in the area of laser tracker error modeling. In particular, they model the non-orthogonality of the axes, zero error in the range, and beam misalignments which they note is the same as collimation error in surveying instruments. Mooring [24] and Zhuang et al. [25] identify errors associated with the beam steering mirror as a significant problem and present a model of these error sources. Loser and Kyle [26] provide a geometrical error model for a laser tracker with a beam steering mirror while Muralikrishnan et al. [27] extend this model for trackers without a beam steering mirror. Lin and Lu [28] present a ray tracing method to model a tracker while Conte et al. [29] describe a kinematic model using D-H notation.

Laser tracker measurements suffer from larger errors in the measurement of angles than along the radial direction. Several researchers have attempted to model errors along the angular axes. Ouyang et al. [30] use a CMM to calibrate the angular axes, Gassner and Ruland [31] and Martin and Chetwynd [32] describe a method to test the angular axes using a precision rotary table, Ginotis et al. [33] present a method for calibration of the vertical angle encoder of spherical coordinate systems in general, Muralikrishnan et al. [34] present a method to determine scale errors in the angle encoders of the laser tracker using an un-calibrated length artifact, Lewis et al. [35] use a network method for angle error estimation, and Nasr et al. [36] compare the different methods.

2.4. Geometrical error models

Understanding the impact of systematic sources of error allows the construction of geometrical error models that can, in turn, be used to improve measurement accuracy. Here, we review geometrical error models for two mechanical constructions of laser trackers – those with a beam steering mirror, and those without.

It should be noted that many sources of error are sensitive to front-face back-face (also known as two-face, front-sight back-sight or plunge-reverse) measurements. That is, if a stationary target is measured in the front-face of the tracker and again in the back-face, the two measurements yield slightly different coordinate values; in the case of an ideal laser tracker construction, the two coordinate measurements should be identical. By measuring several targets distributed in the work volume in both front- and back-face, we can estimate the magnitude of those sources of error that are sensitive to two-face testing. Averaging front- and back-face measurements will eliminate these systematic sources of error; this tactic is commonly used to obtain higher accuracies if required. Both Loser and Kyle [26] and Muralikrishnan et al. [27] note that some of the terms in the model are sensitive to two-face testing.

Table 1
Model parameters for trackers with a beam steering mirror.

Parameter	Description	Two-face sensitivity
$O1x$, $O1y$	Beam offset	No
Ix, Iy	Beam tilt	No
$O2x$, $O2y$	Cover plate offset	Yes
Ex, Ey	Horizontal angle encoder offset	Yes
Kx, Ky	Vertical angle encoder offset	Ky is sensitive, Kx is not
e	Transit offset	Yes
f	Mirror offset	No
i	Transit tilt	Yes
c	Mirror tilt	Yes
j	Vertical index offset	Yes

The geometrical model for a tracker with a beam steering mirror as given by Loser and Kyle [26] is shown in Eqs. (1)–(3). The terms are described in Table 1. In the model, Rm, Hm, and Vm are the measured range, horizontal angle, and vertical angle, respectively, and Rc, Hc, and Vc are the corresponding corrected quantities. The terms $Hoff$ and $Voff$ come from internally corrected PSD measurements and provide a correction when measuring moving reflectors. The vertical index offset j is directly applied when reading the angle and therefore does not appear in the model.

$$Rc = Rm - 2\sin\left(\frac{Vm}{2}\right)\left(e\cos\left(\frac{Vm}{2}\right) + f\right) \tag{1}$$

$$\begin{aligned} Hc = Hm &+ \left(\frac{1}{\sin Vm}\right)\left(Ix\cos Hm - Iy\sin Hm + \frac{O1x\cos Hm - O1y\sin Hm + O2x + Hoff}{Rm}\right) \\ &- \frac{i\sin\left(\frac{Vm}{2}\right) + c}{\cos\left(\frac{Vm}{2}\right)} + Ey\sin Hm - Ex\cos Hm \end{aligned} \tag{2}$$

$$\begin{aligned} Vc = Vm &- (Ix\sin Hm + Iy\cos Hm) \\ &- \frac{O1x\sin Hm + O1y\cos Hm + O2y + Voff}{Rm} \\ &- \cos\left(\frac{Vm}{2}\right)\left(\left(\frac{2}{Rm}\right)\left(e\cos\left(\frac{Vm}{2}\right) + f\right) + Kx\right) \\ &+ Ky\sin\left(\frac{Vm}{2}\right) \end{aligned} \tag{3}$$

The model for trackers without a beam steering mirror as presented by Muralikrishnan et al. [27] is given by Eqs. (4)–(6). The terms are described in Table 2. In the model, Rm, Hm, and Vm are the

Table 2
Model parameters for trackers without a beam steering mirror.

Parameter	Description	Two-face sensitivity
x_{1t} and x_{1m}	Beam offset	Yes
x_2	Transit offset	Yes
x_3	Vertical index offset	Yes
x_{4t}	Beam tilt	Yes
x_5	Transit tilt	Yes
x_{6x} and x_{6y}	Horizontal angle encoder offset	Yes
x_{7n} and x_{7z}	Vertical angle encoder offset	x_{7n} is sensitive, x_{7z} is not
x_8	Bird-bath error	No
x_9 and x_{10}	Second order scale errors in the encoders	No

measured range, horizontal angle, and vertical angle, respectively, and Rc, Hc, and Vc are the corresponding corrected quantities.

$$Rc = Rm + x_2 \sin Vm + x_8 \tag{4}$$

$$Hc = Hm + \frac{x_{1t}}{Rm \sin Vm} + \frac{x_{4t}}{\sin Vm} + \frac{x_5}{\tan Vm} + x_{6x} \cos Hm - x_{6y} \sin Hm + x_{9a} \sin(2Hm) + x_{9b} \cos(2Hm) \tag{5}$$

$$Vc = Vm - \frac{x_{1m}}{Rm} + \frac{x_2 \cos Vm}{Rm} + x_3 + x_{7n} \cos Vm - x_{7z} \sin Vm + x_{10a} \sin(2Vm) + x_{10b} \cos(2Vm) \tag{6}$$

2.5. Compensation

Modern laser trackers routinely incorporate a geometrical error model whose parameters are estimated through a compensation procedure performed in-situ. These procedures depend on the underlying model itself and typically involve front-face back-face measurements and sometimes, the use of a calibrated length. While these procedures are specific to the manufacturer, they share some similarities:

- The constant and length dependent error parameters *A* and *B* of the ADM are obtained by comparing the displacement recorded by the ADM against an IFM over several target positions in its range
- The *R*0 parameter is determined through an inside–outside (buck-in buck-out) test. Two nests are placed on stands a few meters apart. The tracker is placed in line but outside the nests. The tracker's IFM is used to calibrate the inter-nest distance. The tracker is then moved in line and inside the nests and the inter-nest distance is measured using the IFM. Half the difference between these two measurements is assigned as the *R*0 error.
- Several model parameters such as squareness error and beam pointing error (beam tilt) are sensitive to front-face back-face testing. Compensation procedures therefore call for measuring targets located at different heights, azimuths, and distances in front-face and again in back-face. Model parameters are then evaluated by fitting the geometrical model to the observed front-face back-face differences.
- Parameters not captured from front-face back-face tests are determined using measurements made on calibrated artifacts.

Loser and Kyle [26] describe a compensation procedure for one design of a laser tracker. Sawyer and Fronczek [10] discuss a method based on the measurement of calibrated lengths while Hughes et al. [37] describe a network based method for parameter estimation.

2.6. Targets

Laser trackers require a cooperative target to return the beam back to the instrument. Targets used are typically corner-cube reflectors and cat's eye reflectors. Steffey [38] provides an overview of the different targets used and a description of associated error sources. Corner-cube reflectors mounted in a hollow sphere, referred to as spherically mounted retro-reflectors (SMRs), are perhaps the most commonly used reflectors in practice (Fig. 2(a)). These corner-cube reflectors are either constructed of a single piece of solid glass or made of individual glass panels, Fuss et al. [39] discuss the manufacture of SMRs. In both cases, SMRs suffer from three types of error sources: vertex centering error, dihedral-angle error, and polarization error. Vertex centering error is the distance between the optical center and the mechanical center of the SMR; the centering error can be both radial and lateral with respect to the incident laser beam. Centering accuracies are as small as ±2.5 μm in some commercial SMRs currently available. In an ideal SMR, the angle between any two of the three mirror faces is exactly 90°. In reality, these angles may differ by a few arc-seconds, which is the dihedral angle error, resulting in the reflected beam returning in a direction that is not parallel to the incident beam. The dihedral angle errors on some commercially available targets are as small as 1 arcsecond. Large reflectors have panels that are matched for polarization. If there is polarization mismatch, the interferometric pattern may not be created properly. These error sources are described in Refs. [40,41].

While solid glass reflectors suffer from vertex centering and dihedral angle errors, they also suffer from a pointing error due to an apparent shift in the apex position and a range error due to refraction of the beam within the solid glass prism [8]. The solid glass SMRs, however, have a larger acceptance angle, ±40°, in comparison to the ±25° acceptance angle of open-air reflectors. Ouyang et al. [43] study the influence of incident angle on measuring accuracy, noting that while corner-cube reflectors may function for incident angles up to ±35°, it is necessary to maintain the incident angle within ±20° to satisfy laser tracker manufacturer specifications. The spherical form of the housing of high quality SMRs is generally on the order of 1 μm or better (based on NIST internal measurements on 20 commercial SMRs); however, form deteriorates rapidly near the lip. Care must therefore be taken to ensure that the SMR contacts the object being measured at a location away from its lip during a measurement.

While dynamic measurements are generally performed with the operator holding the SMR in his hand, static measurements are performed with the SMR mounted stably on a magnetic nest. There are also several SMR adaptors commercially available that allow the measurement of hole location, axis of a hole, edges, etc. A hole offset adaptor, shown in Fig. 2(e), consists of a magnetic nest to hold the SMR and a shank that is inserted into a hole. The offset distance between the center of the SMR and the top surface of the hole is specified by the manufacturer. Whereas an SMR by itself might not be suitable for measurement of a hole location, adaptors allow such measurements to be performed thus extending the scope and applicability of laser tracker measurements.

One of the challenges of using an SMR in a measurement task is the need to always point it towards the tracker. An active target employs a standard SMR mounted on a two-axis motorized unit that automatically orients itself to point at the tracker at all times. This automatic reorientation is particularly convenient for certain automated tasks such as machine tool error mapping where it can be extremely time-consuming to manually re-orient the target towards the tracker during a measurement [44]. Other targets, referred to as repeatability targets (Fig. 2(b)) consist of corner-cubes that are *not* mounted in a hollow sphere, i.e., are not SMRs. As the name implies, these targets are used to assess the repeatability

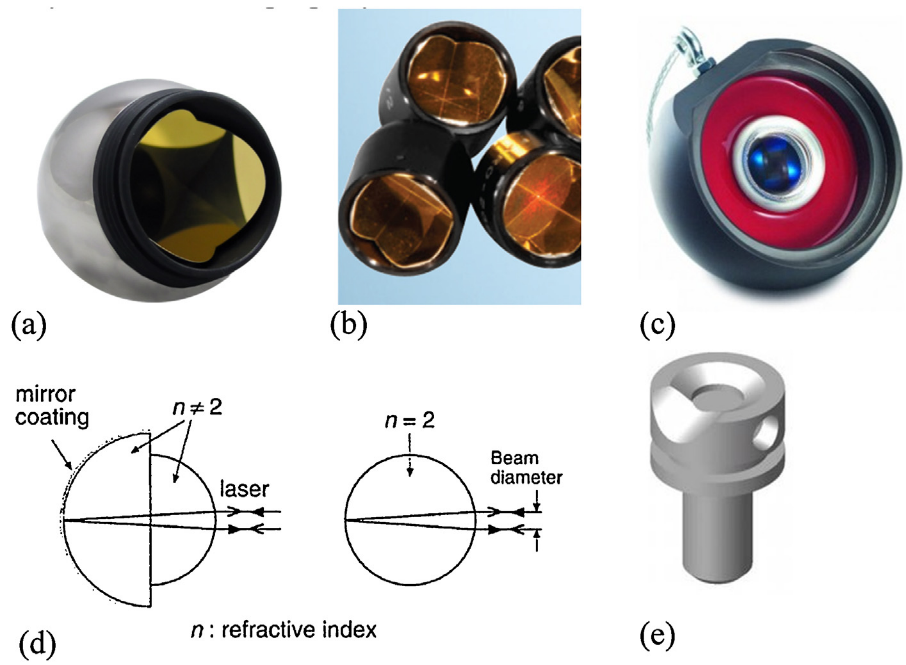

Fig. 2. (a) A corner-cube SMR, (b) repeatability targets, (c) a cat's eye reflector, (d) structure of a conventional ($n \neq 2$) and $n=2$ cat's eye reflector [*Source*: Takatsuji et al. [42], *Meas Sci Technol.* 1999;10(7):N87-N90, ©IOP Publishing. Reproduced with permission. All rights reserved], (e) offset adaptor for hole location measurement.

in tracker measurements or to measure the fixed coordinates of a structure; they are not intended for measurements requiring movement of the corner-cube over the workpiece.

A cat's eye reflector is a passive optical system consisting of a secondary mirror placed at the focal point of a primary lens [45]. In practice, the cat's eye consists of two glass hemispheres of different radii r_1 and r_2, where $r_1=(n-1)r_2$, and n is the refractive index of glass (Fig. 2(c) and (d)). If the refractive index of the glass is not equal to 2, the spheres have different radii, as shown in Fig. 2(d). In that case, the hemisphere on the front has a smaller radius and focuses the incoming parallel beam from the tracker onto the surface of the larger rear hemisphere. The outer surface of the rear hemisphere has a reflective coating that reflects the beam back on a path parallel to the incident beam prior to entering the target. If the refractive index of glass is 2, then the radii of the two hemispheres are equal; in other words, a single sphere of refractive index 2, is by itself, the target as shown in Fig. 2(d). One complication of the $n=2$ sphere is that less than 10% of the incident laser power striking the sphere is returned; in contrast, a Cat's eye returns the majority of the power because of its mirrored coating. Cat's eye targets can provide an acceptance angle of up to 120°, which is two times larger than the acceptance angle of a standard SMR. The design of the cat's eye reflector, optical aberrations, and improvements are discussed in Refs. [42,46–50].

2.7. Hand held accessories

There are several applications that involve the measurement of small features located in large structures; in these applications, a stylus, similar to those used on CMMs, is attached to a hand-held unit and is often a preferable alternative to an SMR. Early designs of such hand-held accessories involved reflecting the laser off of a plate to a corner cube that is attached to the plate and located at a virtual point, which is an equal distance from the plane of reflection as the probe tip. When the laser is locked onto the SMR, the probe tip is aligned along the radial direction (Fig. 3). Misalignment errors in the retro-probe are discussed by Liu et al. [51]. Parker [52] surveys retroreflector designs and propose a novel multidirectional reflector with a virtual point that can be used for measuring points that are hidden from the tracker's line of sight.

Hand-held accessories are increasingly becoming more sophisticated. Today, the hand-held unit typically contains a retroreflector whose apex represents the position of the unit with respect to the laser tracker. The orientation of the unit, determined by the measurement of three angles, along with known probe offset information (probe to SMR apex distance) is then used to determine the coordinates of the probe tip relative to the laser tracker. These hand-held units can also incorporate a laser scanner, not just a touch probe, to facilitate higher data density.

One design of the hand-held unit contains a cluster of LEDs around an SMR. A camera mounted in the laser tracker captures images of these LEDs. The flashing rate of the individual LEDs can be used to uniquely identify them and hence determine the relative orientation of the hand-held unit. The schematic for such a concept is shown in Fig. 4(a) [53]. Another design of the hand-held unit contains a small aperture at the apex of the SMR, thus allowing some portion of the beam to pass through to a CCD array behind the SMR. The position of the spot on the CCD allows the determination of pitch and yaw. Roll is determined using an inclinometer [44]. More recently, Gordon et al. [54] have reported on a touchless pixel probe laser tracker accessory (Fig. 4(b)) as a means of performing non-contact measurements on hard to reach or fragile surfaces. A single pixel in each of three cameras is linked to the laser tracker. The three pixels define a point in space. The orientation of the unit itself is determined though several SMRs mounted on its base.

These hand-held accessories greatly increase the scope and applicability of laser trackers. Hand-held accessories and 6DOF measurements are ongoing areas of research. Kyle [53,55,56] describes recent work in these areas.

3. Multi-station measurements

As mentioned in Section 2, laser tracker measurements suffer from larger errors associated with the rotational axes than along the radial direction. This is a fundamental limitation of measurements made using a single laser tracker. To improve measurement

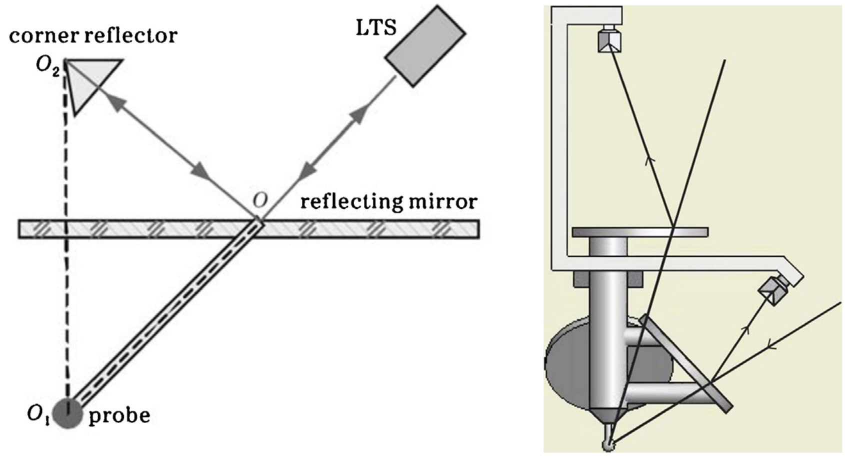

Fig. 3. (a) A retro-probe [*Source*: Liu et al. [51], reproduced with permission from Chinese Optics Letters], (b) hidden point probe with two plane mirrors and two reflectors that allow for simultaneous tracking of the hand-held unit from two different trackers [*Source*: Parker [52], reproduced with permission from Elsevier].

accuracy, measurements from multiple station locations are sometimes combined to obtain more reliable estimates of target coordinates. Such 'averaging' or 'sensor-fusion' methods are the focus of this section.

3.1. Bundle adjustment

Consider a collection of n targets distributed and fixed in space. Let us suppose that these targets are measured from a set of m tracker positions; these measurements can be achieved by m trackers or sequentially by a single tracker from m positions. Each tracker measures the coordinates (x, y, z) of each of the n targets, producing m sets of n-triplets. It is desirable to combine measurements from the m coordinate systems (each corresponding to a tracker position) into a single set of coordinates for the n targets, in a common coordinate frame. Such a frame could be attached to the part or to one of the trackers.

A simplistic approach to this problem involves determining suitable rotation and translation matrices that can transform the data from each of the m tracker positions onto to the coordinate frame of one tracker position. This coordinate transformation can be achieved via least-squares fitting procedures. Fig. 5(a) and (b) depict, respectively, the measurement of a set of 4 targets from 2 tracker positions, and the rigid body transformation to rotate and translate the measurements from position 2 to the coordinate system of position 1. Because the combined measurements average over the systematic errors from both tracker positions, the result is generally more accurate than the same number of repeated measurements from a single tracker.

While rigid body transforms are 'averaging' methods for evaluating target coordinates, 'sensor-fusion' or 'bundle-adjustment' methods are somewhat more complex. Bundle adjustment is a standard photogrammetric technique; Calkins [57] discusses its application in LSDM. This technique involves estimating the optimal tracker *and* target positions through a least squares minimization procedure. This is done by adjusting the position of the trackers and targets until the sum of the squared residuals is minimized. Fig. 5(c) shows the residuals for a tracker along the horizontal angle and ranging direction (residuals along vertical angle direction are not shown, but are typically included in the minimization procedure). These residuals are determined from current estimates for tracker and target locations. Similar residuals are estimated for each target-tracker pair. The bundle-adjustment algorithm then perturbs the tracker and target locations to evaluate the next set of estimates for target and tracker locations. This process is repeated until the sum of squared residuals is minimized. Bundle adjustment methods typically use weights to reduce the influence of errors associated with angle measurements, as discussed by Sandwidth and Predmore [58] in the context of laser tracker measurements. In the limiting case of assigning zero weight for angle measurements, the bundle adjust solution converges to the multilateration solution; multilateration is discussed in the

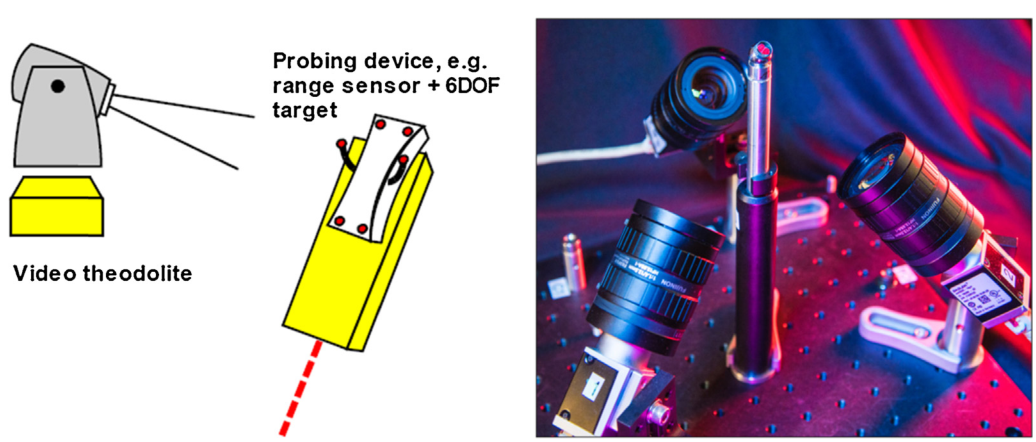

Fig. 4. (a) Hand-held accessory containing several LEDs is shown [*Source*: Kyle [53], reproduced with permission from Stephen Kyle and CMSC]. A camera on the laser tracker (a video theodolite is shown in the figure instead of a tracker) monitors the LEDs to determine the orientation of the unit, (b) pixel probe [*Source*: Josh Gordon, NIST].

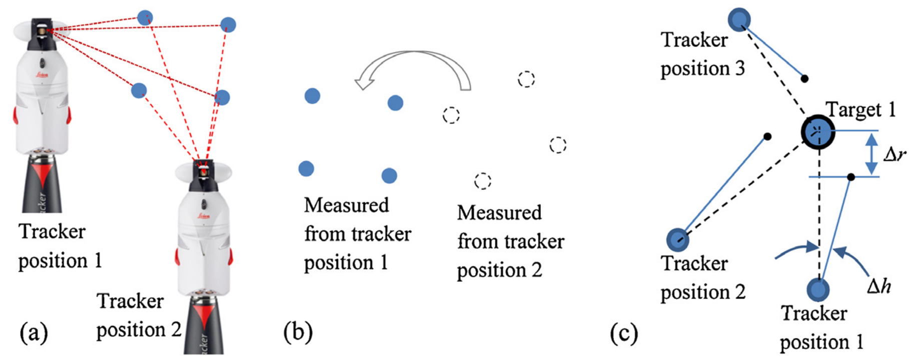

Fig. 5. (a) Two laser trackers measuring a set of 4 targets, (b) transforming the coordinates from position 2 to position 1 via rigid body transformation, (c) residuals shown for a planar case for bundle-adjustment [*Source*: all parts are original illustration by authors].

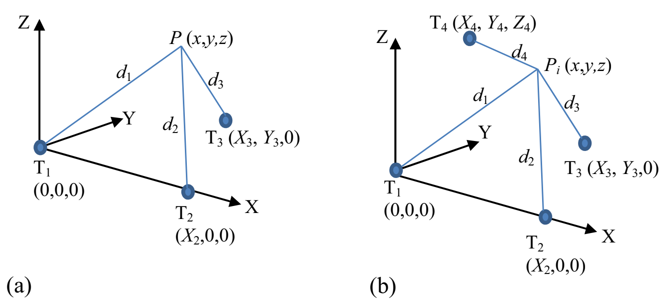

Fig. 6. (a) Trilateration and (b) multilateration with four trackers [*Source*: both parts are original illustration by authors].

next section. Dynamic weighting, different merit functions, and accounting for uncertainty ellipsoids, are discussed in Refs. [59–62].

3.2. Multilateration

While bundle adjustment uses range and angle information from multiple station positions, it is possible to obtain coordinates with high accuracy using only range information from each station. The theoretical framework for this is well-established. The technique is referred to as trilateration when three stations are used or, more generally, multilateration. In the simple case of trilateration (Fig. 6(a)), the tracker positions are assumed to be known relative to each other. Without loss of generality, one of the trackers can be assumed to be at the origin of the coordinate system. The position of a second tracker defines the x axis, i.e., the second tracker is located at a known distance X_2 on that axis. The third tracker is assumed to be at a known coordinate on the xy plane, (X_3, Y_3). The coordinate (x, y, z) of the target P can then be determined from the following system of three equations

$$x^2 + y^2 + z^2 = d_1^2 \tag{7}$$

$$(x - X_2)^2 + y^2 + z^2 = d_2^2 \tag{8}$$

$$(x - X_3)^2 + (y - Y_3)^2 + z^2 = d_3^2 \tag{9}$$

The previous equations consist of three knowns: d_1, d_2, and d_3, which are the three measured ranges from each of the trackers. It is generally not feasible to calibrate tracker locations relative to each other. The addition of a 4th tracker along with more target locations results in more known parameters than unknown parameters, thus allowing for simultaneous determination of target and tracker positions. In Fig. 6(b), there are 6 unknown parameters associated with the position of the 4 trackers and 3 unknown parameters associated with each target P_i. There are 4 known distances associated with each target P_i (one known distance from the target to each of the 4 trackers). If there are 6 targets, there are 24 unknown parameters and 24 known parameters. Thus the coordinates of the 6 targets can be determined along with the coordinates of the trackers. This self-calibration, i.e., the ability to determine tracker locations thereby establishing the metrology frame in-situ, is key to realizing multilateration in practice. The use of more than 6 targets (with 4 trackers) provides redundancy, thus improving the accuracy in the detection of target coordinates.

Early work in the area of coordinate metrology using length measurements was reported by Nakamura et al. [63]. The authors use a two-beam tracking interferometer for in-plane measurements where the distance between stations has been calibrated previously. Nakamura and Goto [64,65] expand on this work by incorporating three and four beam laser interferometry to determine 3D coordinates of a small travel stage; it should be noted, however, that this work does not use tracking interferometry. Rather, the beam directions are fixed. Fixed beam directions are feasible because the stage motions are small in comparison to beam width. The direction vectors of the beam along with target position are determined simultaneously in a self-calibrating manner. Takatsuji et al. [66] describe the first measurement of a 3D coordinate using four laser tracker stations to simultaneously determine target and tracker locations in a self-calibrating scheme. Takatsuji et al. [67,68] provide a set of four equations to solve the multilateration problem:

$$x^2 + y^2 + z^2 = d_1^2 \tag{10}$$

$$(x - X_2)^2 + y^2 + z^2 = d_2^2 \tag{11}$$

$$(x - X_3)^2 + (y - Y_3)^2 + z^2 = d_3^2 \tag{12}$$

$$(x - X_4)^2 + (y - Y_4)^2 + (z - Z_4)^2 = d_4^2 \tag{13}$$

Substituting Eq. (10) into Eqs. (11)–(13), we get

$$-2\begin{bmatrix} X_2 & 0 & 0 \\ X_3 & Y_3 & 0 \\ X_4 & Y_4 & Z_4 \end{bmatrix}\begin{bmatrix} x \\ y \\ z \end{bmatrix} = \begin{bmatrix} d_2^2 - d_1^2 - X_2^2 \\ d_3^2 - d_1^2 - X_3^2 - Y_3^2 \\ d_4^2 - d_1^2 - X_4^2 - Y_4^2 - Z_4^2 \end{bmatrix} \tag{14}$$

Takatsuji et al. [67,68] show that Z_4 cannot be zero for the existence of the inverse of the coefficient matrix on the left hand side of Eq. (14). That is, for the multilateration problem to be solved, a fourth laser tracker must not occupy the plane defined by the other three trackers.

While uncertainty in an individual laser tracker's range measurements may be small, i.e., on the order of a few micrometers, the uncertainty in a measured point coordinate can be considerably large in some instances. The increased uncertainty can be a result of non-optimal measurement geometry; a 2D example is presented in Fig. 7(a). Consider two trackers T_1 and T_2 located at a known

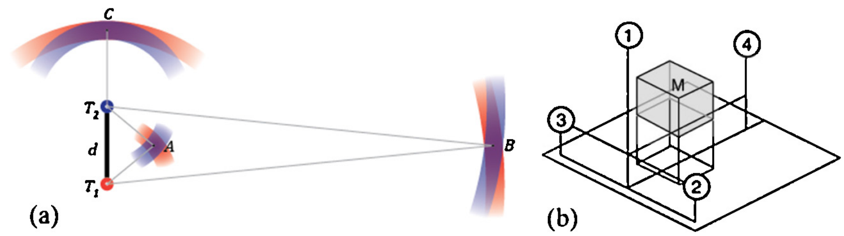

Fig. 7. (a) Region of uncertainty for three targets [*Source*: original illustration by authors], (b) an equilateral-tetrahedron arrangement of trackers (1–4) with the measurement volume M enclosed by the trackers [*Source*: Takatsuji et al. [69], *Meas Sci Technol*. 2000;11(5):477-483, ©IOP Publishing. Reproduced with permission. All rights reserved].

distance *d* from each other. Let us suppose that there is some uncertainty in the range measurements to each of three targets from the two trackers. That uncertainty is shown as an annular region centered on the nominal target position. The region of overlap between the annuli from the two trackers is the region of uncertainty in the target coordinate. The two annuli for target A intersect in such a manner as to provide a small uncertainty zone. In the case of targets B and C, the ranging axes of the trackers are parallel or nearly parallel, resulting in the two annuli intersecting to produce a large uncertainty zone. For the case of 3D multilateration measurements, Takatsuji et al. [69] show that the measurement error is smallest when the trackers are placed in a tetrahedral arrangement and the targets are enclosed by the trackers, see Fig. 7(b). While Fig. 7(a) provides a qualitative picture of the importance of geometry on errors, Zhang et al. [70] provide a quantitative formulation for measurement error σ as a product of a magnification factor k and the uncertainty in range measurement σ_l, where the factor k is related only to geometry of the measurement. This effect arises in numerous metrology situations, in Global Positioning System (GPS) measurements it is known as Geometric Dilution of Precision (GDOP) [71]. Much of the research on multilateration is focussed on understanding and optimizing the geometry of the problem and in quantifying errors in the measured coordinates [72–76].

3.3. The laser tracer and other tracking interferometers

While a laser tracker can be used in a multilateration scheme to determine coordinates of points in space, error motions associated with the rotational axes within the instrument can impact the accuracy of range measurements. In order to address this issue, researchers at the National Physical Laboratory (NPL) and the Physikalisch-Technische Bundesanstalt (PTB) designed the laser tracer [5,77] (see Fig. 8). The laser tracer consists of a high quality sphere within a dedicated optical arrangement that allows the sphere center to serve as the reference for all interferometry measurements. Muralikrishnan et al. [78] compare the radial error motions of a laser tracer and three different laser trackers and show that the radial error motions of the laser tracer are in fact smaller than those of trackers. The laser tracer only reports range, not angles, and can therefore only be used in a multilateration mode. Other researchers have also noted that early laser trackers were bulky and not sufficiently accurate to perform multilateration, and have therefore developed their own tracking interferometers [79,80].

3.4. Applications of multilateration in LSDM

The 21 parametric errors of a CMM have historically been estimated using traditional (fixed) laser interferometry and/or calibrated artifacts such as step gages, ball plates, etc. Wendt et al. [81] first reported the use of laser trackers in a multilateration scheme for CMM error mapping. In that article, the authors use a single tracking station that is moved sequentially to multiple positions on the table. The technique relies on the repeatable positioning of the reflector at the same points in space between one tracking station location to the next. The use of single and/or multiple stations for CMM error mapping has since been explored by others [77,82–84]. Multilateration has also been used for error mapping numerically controlled (NC) machine tools [85–88] and more recently, to determine parameters of articulating arm coordinate measuring machines (AACMMs) [89].

4. Performance evaluation, standards, traceability, and uncertainty

With general acceptance and use of laser trackers in industry in the late 1990s and early 2000s, the need for establishing standardized performance testing protocols became evident. Ruland [90] describes a series of performance tests on a laser tracker as early as 1992. In a report to the Coordinate Metrology Systems Conference (CMSC) in 1996, Caskey et al. [91] address the issues of traceability and measurement uncertainty of laser tracker measurements, and how these topics relate to standards development. It was realized early on that the testing philosophy of a laser tracker will be similar to that of CMMs to the extent that reference lengths can be measured in different portions of the work volume to assess

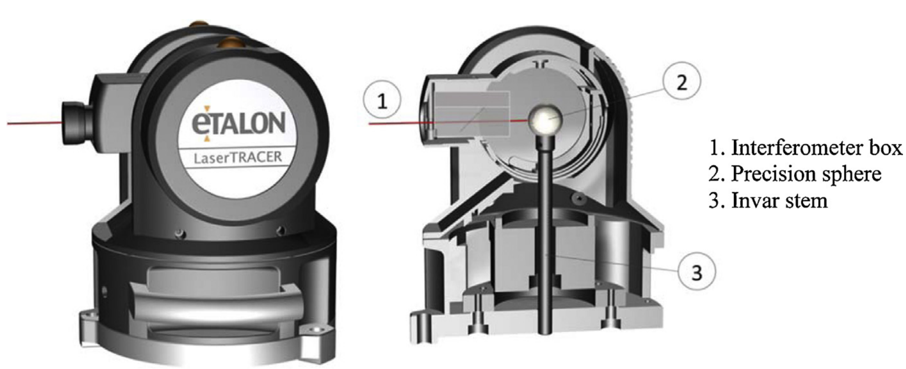

Fig. 8. Schematic of the laser tracer [*Source*: Heinrich Schwenke, Etalon AG, Germany].

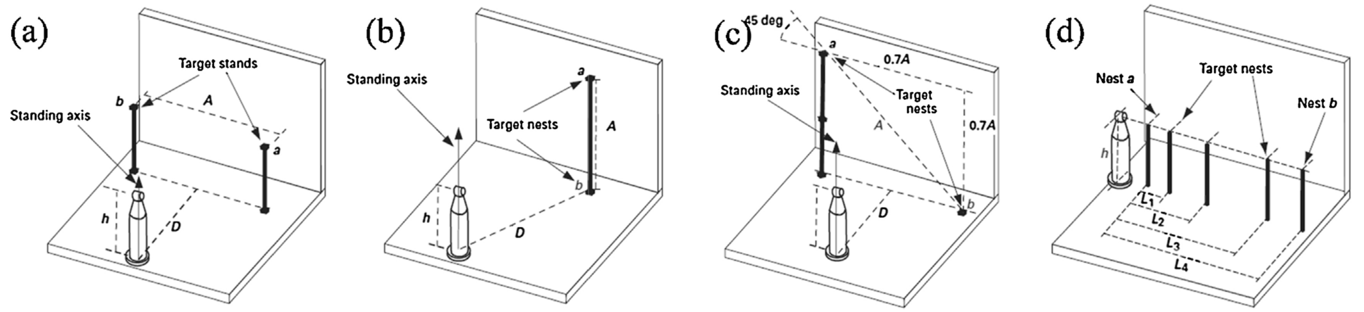

Fig. 9. ASME B89.4.19 tests. (a) Horizontal length test, (b) vertical length test, (c) left diagonal length test, and (d) ranging tests [*Source*: All parts reprinted from ASME B89.4.19-2006 [40], by permission of The American Society of Mechanical Engineers. All rights reserved].

the performance of the instrument. However, unlike a Cartesian CMM with 21 parametric errors, the construction of the tracker and, therefore, the nature of the error sources are different. The performance of the radial axis of the laser tracker is independent of the mechanical behavior of the instrument and therefore can be tested separately. It was discussed in Section 2.3 that the angular axes are the primary contributors to volumetric errors; therefore, test procedures to assess volumetric performance should be sensitive to these error sources. Early calls for standardization by Clarke et al. [92,93] and Sawyer et al. [94] recognize the importance of testing a laser tracker along directions that are sensitive to the different error sources. While Clarke et al. [92,93] use a scale bar for performance testing, Sawyer et al. [94] propose the use of a laser rail system. Regardless of how the reference lengths are realized, the use of calibrated lengths in different portions of the work volume is also the general philosophy of the test procedures in published and draft standards [40,95,96]. We briefly describe these performance standards and other related topics, such as scale bar development and traceability, next.

4.1. ASME B89.4.19

There are three broad classes of tests in the ASME B89.4.19 [40]: ranging performance tests, two-face tests, and volumetric length tests. There are 35 different combinations of calibrated artifact positions and laser tracker orientations in the volumetric tests and 12 different combinations of target location and laser tracker orientation for the two-face tests; each of these test setups have three repeated measurements performed. Additionally, there are five calibrated lengths measured in the ranging test. Two-face tests and volumetric length tests are designed to assess the performance of the angular axes. The standard only describes the test positions and orientations; users are allowed to realize the tests in different ways. Fig. 9 provides a schematic for performing some volumetric tests; in particular, the horizontal length test, the vertical length test, the left diagonal length test, and the different ranging length tests are shown. Sawyer et al. [94], Estler et al. [97], and Muralikrishnan et al. [98] describe the implementation of the ASME B89.4.19 tests using the laser rail system, Ma et al. [99] describe a laser plane, and Nasr et al. [100] describe the use of a scale bar artifact.

While many of the tests described within the ASME B89.4.19 are sensitive to the different sources of geometrical error within laser trackers, Muralikrishnan et al. [27] identify redundant test positions and document systematic errors that were not adequately evaluated, and propose additional tests for increased sensitivity to all error sources. In particular, they point out the benefits of using asymmetric test positions such as the asymmetric horizontal length, asymmetric vertical length, asymmetric diagonal length, and a horizontal length positioned above the tracker, as shown in Fig. 10.

4.2. VDI/VDE 2617-10

The VDI/VDE 2617-10 [95] includes a probe size test, a probe form test, and volumetric length tests. The probe size and form tests are performed by measuring several points on a sphere of calibrated size and form. The volumetric length tests are first performed by placing the tracker in front of a rectangular volume of 10 m × 6 m × 3 m (recommended size). A total of 96 lengths are measured in this volume. The tracker is then moved inside the volume and 9 additional lengths are measured, for a total of 105 lengths. The tracker and the measurement volume are shown in Fig. 11(a). A convenient way to create the testing positions is by projecting the lengths onto a plane and repositioning the tracker as shown in Fig. 11(b).

4.3. Draft ISO 10360-10

The draft ISO 10360-10 [96] includes probe size, probe form, probe location, and volumetric length tests. The probe size and

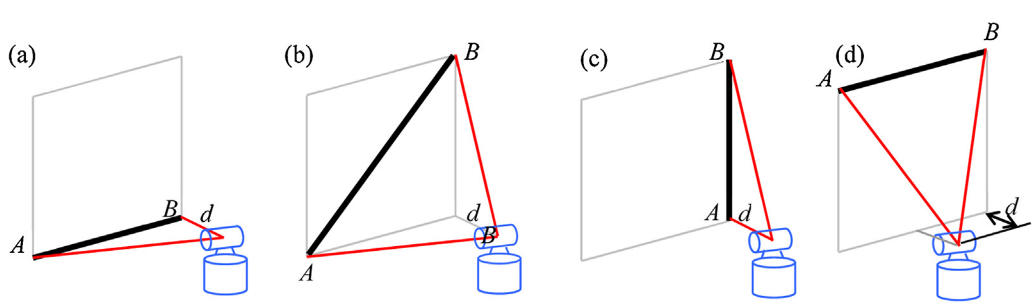

Fig. 10. Asymmetrical and other sensitive tests proposed by Muralikrishnan et al. [101]. (a) Asymmetric horizontal length, (b) asymmetric diagonal length, (c) asymmetric vertical length, and (d) horizontal length above the tracker [*Source*: all parts are original illustration by authors].

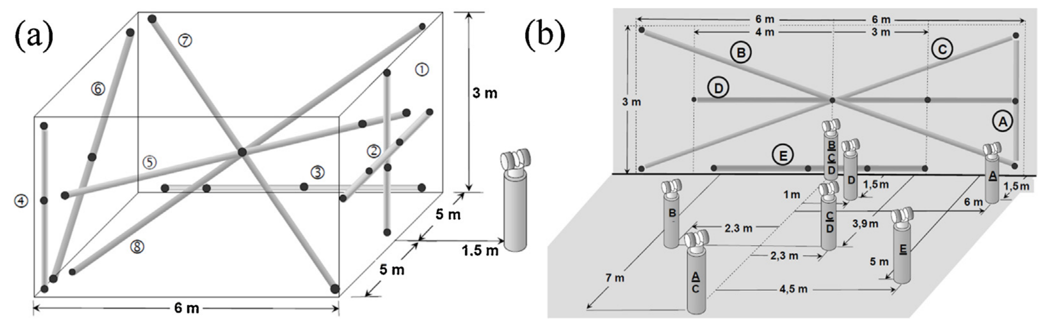

Fig. 11. VDI/VDE 2617-10 tests [95]. (a) Measurement volume showing the tracker and different length positions and orientations, (b) the different length positions and orientations are projected on to a plane. The tracker locations are shown in the figure to realize the different test positions [*Source*: VDI/VDE 2617-10, Reproduced with the permission of the Verein Deutscher Ingenieure e.V].

form tests are performed by measuring 25 points on a sphere of calibrated size and form and evaluating these two measurands. The probe location tests are two-face tests on fixed targets. The volumetric length tests are comprised of two sections – core tests and user-defined tests. There are 41 core tests designed to be sensitive to all known systematic error sources in various tracker designs. The remaining 64 tests are user-defined. There are two default options for these 64 tests – one set is drawn from the ASME B89.4.19 while the other set is drawn from the VDI/VDE 2617-10. The user is also free to choose their own set of 64 user-defined tests. Muralikrishnan et al. [101] present an assessment of the merits and weaknesses of both the ASME B89.4.19 and the VDI/VDE 2617-10 and a description of the test procedures in the draft ISO 10360-10.

4.4. Scale bar

Although there is extensive history in the development and calibration of ball-bars for CMM testing [102–107], the design of scale bars for testing of laser trackers proved to be much more challenging because of their long length and problems associated with mechanical and thermal stability. Phillips et al. [104,107] highlight desirable properties of free standing ball bars and a high-accuracy laser-based ball bar system for large CMMs. Sawyer et al. [108] present a model for change in length of a scale bar due to gravity induced loading. Since the length of the scale bar may vary between the calibration and eventual use, they are generally calibrated in-situ using the IFM of a laser tracker. Hudlemeyer et al. [109] describe the design of one such scale bar and Lee et al. [110] report on a procedure for interim checking of laser trackers using the same bar. The use of calibrated ball-bars that are manually probed with an SMR can be particularly problematic due to the asymmetrical axial and transverse stiffness of the bar resulting in significant length errors as reported by Phillips (in Chapter 9, Hocken and Pereira [9]).

4.5. Metrological traceability

In the previous sections, we discussed published and proposed documentary standards for performance testing of laser trackers. We discuss here how the results from these tests relate to establishing traceability of laser tracker measurements. According to the international vocabulary on metrology (VIM), metrological traceability is the property of a measurement result whereby the result can be related to a reference through a documented unbroken chain of calibrations, each contributing to the measurement uncertainty [111]. The laser tracker is a complex assembly of sub-systems each with their own set of systematic errors. While it may be possible to individually calibrate sub-systems, establishing traceability of the entire assembly is not straightforward. Caskey et al. [91] note the following:

> "it is possible to individually calibrate the laser interferometer, establishing conformance to the SI basic unit of length at a given level of uncertainty. Similarly, the rotary axis angular encoders can be calibrated, using an artifact. . .However, this is not sufficient to constitute traceability of the laser tracker itself".

Metrological traceability involves a series of documentary and technical requirements [112]. While the documentary activities, such as providing calibration certificates as evidence of a traceability chain are straightforward, the technical activity of providing task specific measurement uncertainty for the particular measurand under evaluation is complex and discussed in Section 4.7. If a laser tracker, as a system, can be evaluated through a suite of performance tests, e.g., national or international standards that are sensitive to all of its error sources, those test results can be used to estimate the point coordinate uncertainty. The performance test protocol and resulting values are part of the documentary evidence in the traceability chain. The topic of measurement traceability is addressed by Swyt et al. [113] and Phillips et al. [114].

4.6. Dynamic measurements, time, and temperature

All of the test procedures and documentary standards described earlier only assess the performance of a laser tracker in its static mode of operation. Laser trackers can however also measure in a dynamic mode, i.e., providing the coordinates of a target in motion. In fact, many applications (such as robot performance evaluation) require the use of a tracker in its dynamic mode. Test procedures such as using a target in a linear stage or on a rotary table are described by Lau et al. [44] and Morse et al. [115]. These procedures are still under research and discussion, and not yet under the consideration of standards committees. Dynamic weighting models to improve performance have been reported by Liu at al. [116].

Laser tracker performance is affected by the temperature in the environment. While the assumption that light travels in straight lines and at constant speed may be valid in a controlled laboratory environment, it is not necessarily valid in a shop floor environment or outdoors where laser trackers are often used. Estler et al. [7] point out that there are three important effects to consider – bending of light due to gradients in index of refraction, variation in speed of light, and turbulence caused by time dependent variations in refractive index. They note that a 1 K/m gradient in temperature normal to (and continuous over) the beam path will result in the laser beam deviating from the straight line by 50 μm over 10 m of travel. The ASME B89.4.19 also discusses the effect of beam retardation and refraction; Appendix E of the standard presents equations to quantify the errors in the radial and transverse directions due to air temperature effects. In particular, the ASME standard describes a thermal gradient that varies along the beam path illustrating the potential errors of a localized heat source, especially one located near the tracker causing an especially long lever arm to magnify the refraction effects. While laser tracker measurements can in principle be corrected for temperature gradients through numerous thermistors distributed in the work volume, it is rarely done so in practice because of the complexity involved. Temperature gradients in the work volume are perhaps one of the limiting constraints in the achievable accuracy of laser trackers today. Sandwith [117] reports on improvements in performance by compensating the tracker on the shop floor while Ouyang et al. [118] study stability of the tracker as a function of time and temperature.

4.7. Uncertainty

A tracker that satisfies a suite of performance verification tests such as the ASME B89.4.19 is considered to be 'in conformance,' i.e., the tracker can be reasonably expected to meet the manufacturer's specification for any measurement within its rated conditions. The results of the test procedure (typically point-to-point length) do not directly provide the user with a measurement uncertainty for the specific measurement being performed. The manufacturer's specifications may be considered as an upper limit on the uncertainty of point-to-point length measurements such as those described in a documentary standard. The determination of the uncertainty for a specific measurement task such as diameter of a cylinder bore, or profile of a free form surface, is a much more complicated problem. All influence factors must be identified and the contribution from each source combined as described in the GUM [119]. This can be a challenging and time consuming activity. The general approach involves determining the point coordinate uncertainties and then propagating those uncertainties into the evaluated measurand. Propagating uncertainty involves knowing the point sampling strategy (number and location of the measured points on the workpiece) and how the points are used to compute the specific result. Monte Carlo methods may be used to numerically estimate the point coordinate uncertainty (which can be extracted from performance test results of standard tests), which are then propagated into the combined and expanded uncertainty of the specific measurand [120–122]. Baldwin et al. [123] present this calculation for CMMs using standardized test results. Forbes et al. [124–126] present a mathematical formulation for calculating the uncertainty in laser tracker measurements based on a simple model of random and systematic errors associated with a measurement. The estimates for the uncertainty in point coordinates are described as explicit functions of the random and systematic effects and the uncertainties are propagated. The variance matrix is shown highlighting the correlation between variables. Huo [127] et al. and Peggs [128] describe virtual technologies for uncertainty estimation; such virtual instruments contain an underlying model along with an uncertainty engine that uses Monte Carlo methods for estimating measurement uncertainty.

Another approach for estimating measurement uncertainty is suggested by Calkins [57] and involves combining measurements from multiple tracker positions. In this approach, redundant data are used to extract some measure of the variability associated with the entire system: the tracker, operators, environment, etc. Fig. 5(c) shows a target measured by three tracker stations. The bundle adjustment procedure optimizes the target and tracker positions to minimize the residuals (shown in Fig. 5 as Δh and Δr). The residuals after bundle adjustment then provide a measure of the uncertainty in the point coordinate. The mathematical formulation for combining measurements from multiple stations is described by Forbes [126,129]. The estimation of uncertainty for point coordinates collected in dynamic mode is a far more complex problem and has been addressed by Ulrich et al. [130,131].

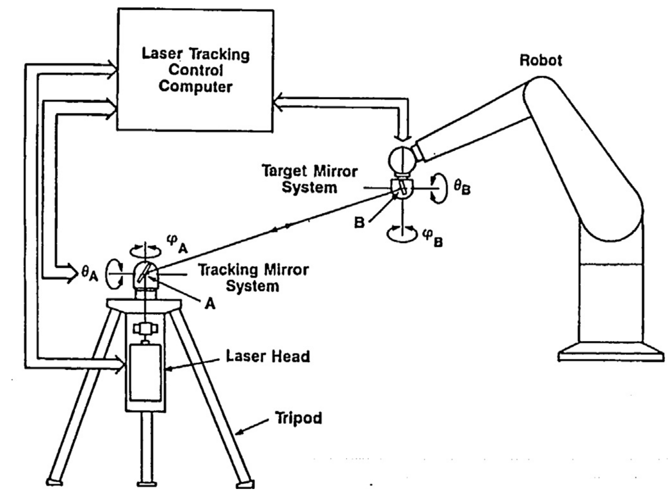

Fig. 12. Laser tracker monitoring robot position and pose [*Source*: Lau [3] et al., reproduced with permission from Elsevier].

5. Applications

Over the last 30 years and, in particular, the last decade, laser trackers have been increasingly used in a wide range of manufacturing and assembly applications. We provide a sample of references that highlight the breadth and complexity of these applications.

5.1. Robot metrology

The driving force behind the development of the laser tracker was the need to "device methodologies, instruments, and standard test procedures for characterizing the accuracy, repeatability and dynamic performance of robots" [2]. Fig. 12 shows the schematic of a laser tracking interferometer reported by Lau et al. [3]. Industrial robots are repeatable but suffer from poor absolute accuracy. Their repeatability, however, allows for the calibration of end-effector errors using external metrology systems such as the laser tracker. While previously, multiple laser tracker measurements were required to obtain pose of the end-effector, a significant recent development is the use of commercially available 6-dof systems (such as those based on the concepts described in Section 2.7) to directly monitor position and pose [132,133]. In fact, the use of 6-dof systems allows for continuous monitoring of the robot even during manufacturing and assembly when thermal variations, loading forces, etc., can cause significant deviations to end-effector position and orientation.

5.2. CMM, AACMM, and machine tool error mapping

Software compensation of geometrical errors is a standard practice to improve the accuracy of CMMs and high-accuracy numerically controlled machine tools. The 21 parametric errors associated with the three linear axes and any additional errors associated with rotational axes are typically individually mapped. This is a labor intensive and time consuming process. As mentioned in Section 3.4, laser trackers in multilateration mode have been used to map geometrical errors in CMMs [77,81–84] and machine tools, resulting in significant savings in time and cost. The approach involves using multiple trackers or a single tracker in sequential mode, to measure the coordinates of a reflector on the ram at numerous locations in the work volume. The CMM coordinates are also recorded at these locations. The different parametric errors are obtained by mathematically fitting polynomial functions to the measured data. Fig. 13(a) shows measurements of the reflector

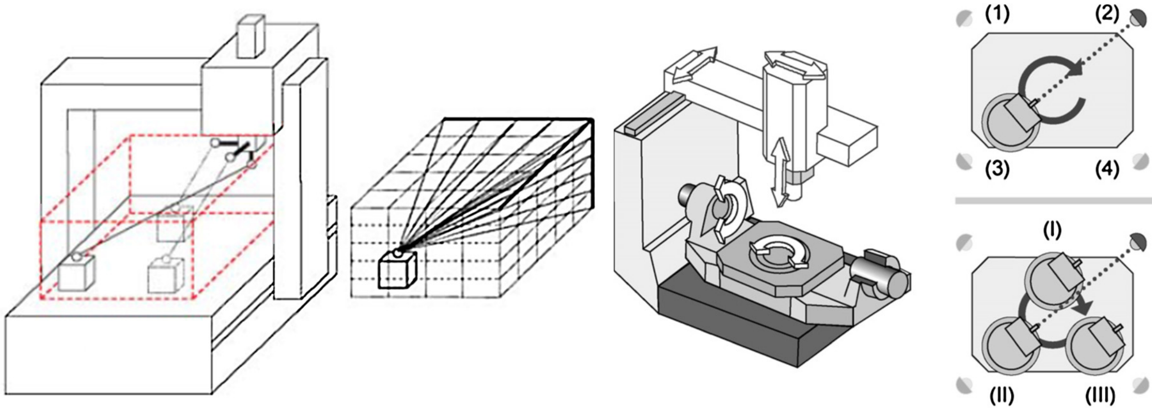

Fig. 13. (a) Estimation of geometrical errors of a CMM from different tracker positions [*Source*: Schwenke et al. [77], reproduced with permission from Elsevier], (b) estimation of rotary table errors using laser trackers in multilateration mode [*Source*: Schwenke et al. [83], reproduced with permission from Elsevier].

from three tracker positions and the spatial grid of points using a single tracker in sequential mode [77]. Fig. 13(b) shows a schematic for the measurement of errors associated with a rotary table using a similar strategy [83]. With the tracker in one of the three stations (I, II, and III), and for each of the four positions (1, 2, 3, and 4) of the reflector, the rotary table is rotated incrementally through a full 360° and the distance is recorded for each sampling point. The data are then used to calculate the different parametric errors of the rotary table. Laser trackers in multilateration mode have also been used to map the errors of numerically controlled machine tools [85–88] and more recently, to estimate parameters of AACMMs [89].

5.3. Reference measurements for the performance evaluation of other devices

The laser tracker is often used to provide reference measurements for the performance evaluation of other lower accuracy metrology devices. Multiple researchers [134–136] have reported using laser trackers to calibrate a grid of targets for the performance evaluation of indoor GPS type distributed systems. The targets are measured with a laser tracker from more than one location. Muelaner et al. [134] use bundle adjustment to combine the laser tracker data to obtain target coordinates with lower uncertainty, while Eger et al. [136] use simulation to obtain best tracker station positions for use in multilateration mode. After the target locations are known, the coordinates of the same targets are then determined using the instrument under test. Point-to-point distances are then compared to assess the performance of the instrument under test. MacKinnon et al. [137] and Ferrucci et al. [138] report on a similar strategy for assessing the performance of large volume laser scanners. Fig. 14 shows a series of kinematic nests mounted on a horizontal rail. The nest-to-nest distances are calibrated using a laser tracker. A laser scanner then measures the same nest-to-nest distance; point-to-point distances are compared to evaluate laser scanner performance.

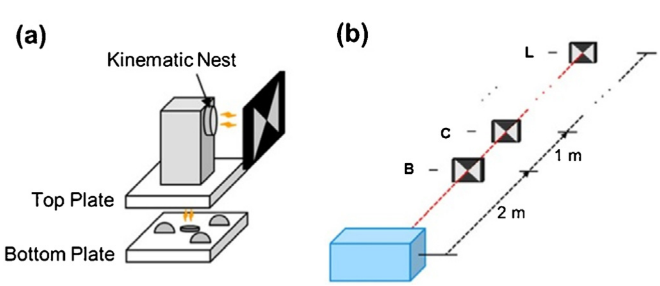

Fig. 14. Test setup to evaluate point-to-point distance performance of laser scanners [*Source*: Ferrucci et al. [138], *Meas Sci Technol*. 2014;25, ©IOP Publishing. Reproduced with permission. All rights reserved].

5.4. Manufacturing and assembly of aerospace components

The long range, high accuracy and relative ease of use of laser trackers have long been recognized as compelling aspects for their adoption in aerospace applications [139,140]. With the publication of documentary standards such as the ASME B89.4.19 and the VDI/VDE 2617-10, metrological traceability of laser tracker measurements are now firmly established, thereby removing any barriers to their adoption in the shop floor. Laser trackers are now used in jig and fixture building, part inspection, joining of large parts for final assembly [141], etc. In typical jig-based assembly, hard tooling is used to locate large aircraft sub-assemblies that are indexed to fixtures. Automated alignment systems such as laser trackers establish soft datum to which aircraft parts are located during assembly [142]. Fig. 15 shows an aircraft wing on motorized positioner located using laser trackers as it is assembled onto the fuselage. The significant advantages of such automated alignment systems include lower investment in fixed tooling, shorter lead time for introduction of design variants, reduced labor cost, improved quality, and flexibility.

5.5. Alignment and measurement

In the area of astronomy, laser trackers are used for aligning optical components, in the manufacture of aspherics, etc [143–145]. In the testing of antenna properties, laser trackers have been used to establish a permanent coordinate system for compact antenna ranges and also to evaluate the surface of parabolic mirrors [146,147]. In the area of high energy physics, laser trackers are again used for complex mechanical and optical alignments. Linear and circular particle accelerators use electric fields to accelerate ions or charged subatomic particles to high speeds while maintaining well-defined trajectories. Alignment requirements are generally on the order of a millimeter over distances ranging from several hundred meters to several kilometers. Martin [148] provides an overview of different techniques and instrumentation in the field of accelerator alignment. Wojcik and Lakanen [149] present an overview of laser trackers applied to survey and alignment problems at Fermilab. The National Ignition Facility (NIF) is a large laser based Inertial Confinement Fusion (ICF) device where beam and target alignment must be performed to very tight specifications. Kalantar et al. [150] survey alignment needs for the NIF.

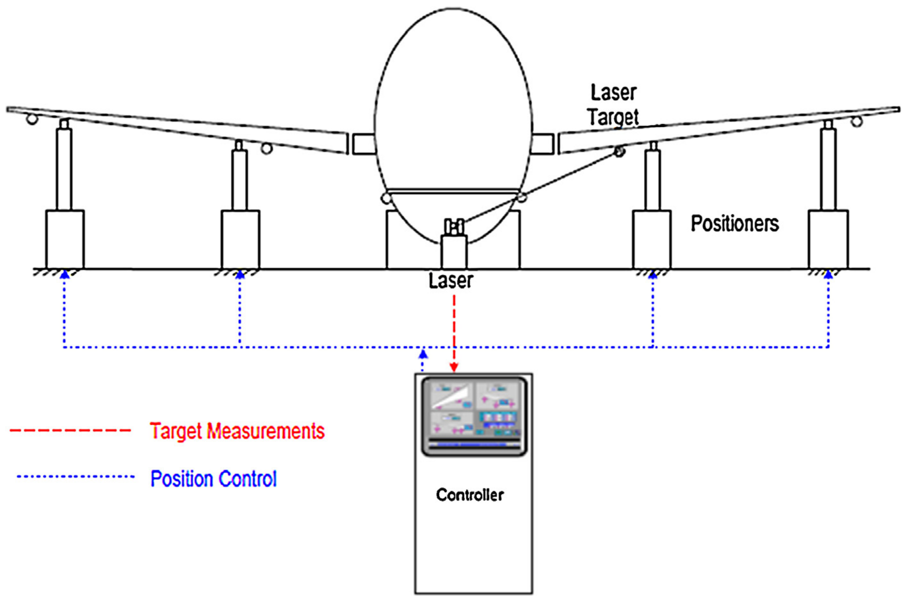

Fig. 15. Aircraft component assembly using automated positioning and alignment [*Source*: Williams et al. [142], reprinted with permission from SAE International].

6. Conclusions

Since the publication of the seminal work by Lau et al. [1,2], a significant amount of research and development has resulted in the evolution of the laser tracker from a tool intended for robot metrology into a highly accurate dimensional metrology tool now widely accepted and in fact, preferred, in a variety of applications including manufacturing, assembly, alignment, etc. In this paper, we have reviewed literature pertaining to laser trackers as applied to dimensional metrology, covering their design, operation, performance evaluation, measurement uncertainty, and applications.

Disclaimer

Commercial equipment and materials may be identified in order to adequately specify certain procedures. In no case does such identification imply recommendation or endorsement by the National Institute of Standards and Technology, nor does it imply that the materials or equipment identified are necessarily the best available for the purpose.

Acknowledgements

The authors thank Dr. Kam Lau, Massimiliano Ferrucci, Christopher Blackburn, and Prem Rachakonda for carefully reviewing the manuscript.

References

[1] Lau K, Hocken R, Haynes L. Robot performance measurements using automatic laser tracking techniques. Robot Comput Integr Manuf 1985;2(3/4):227–36.
[2] Lau K, Hocken R, Haight W. An automatic laser tracking interferometer system for robot metrology. In: 3rd International Precision Engineering Seminar. 1985. p. 100–2.
[3] Lau K, Hocken RJ, Haight WC. Automatic laser tracking interferometer system for robot metrology. Precis Eng 1986;8(1):3–8.
[4] Slotwinski T, Blanckaert P. Frequency modulated coherent laser radar technology. In: Proceedings of the OPTIMESS2007 Workshop. 2007. p. 386–91.
[5] Hughes EB, Wilson A, Peggs GN. Design of a high-accuracy CMM based on multi-lateration techniques. CIRP Ann – Manuf Technol 2000;49(1):391–4.
[6] Peggs GN, Maropoulos PG, Hughes EB, Forbes AB, Robson S, Ziebart M, et al. Recent developments in large-scale dimensional metrology. Proc Inst Mech Eng Part B: J Eng Manuf 2009;223(B6):571–95.
[7] Estler WT, Edmundson KL, Peggs GN, Parker DH. Large-scale metrology – an update. CIRP Ann – Manuf Technol 2002;51(2):587–609.
[8] Harding K, editor. Handbook of optical dimensional metrology. CRC Press; 2013.
[9] Hocken R, Pereira P, editors. Coordinate measuring machines and systems. 2nd ed. CRC Press; 2011.
[10] Sawyer DS, Fronczek C. Laser tracker compensation using displacement interferometry. In: Proceedings of the ASPE 18th Annual Meeting. 2003.
[11] Edlén B. The refractive index of air. Metrologia 1966;2(2):71–80.
[12] Birch KP, Downs MJ. An updated Edlén equation for the refractive index of air. Metrologia 1993;30(3):155–62.
[13] Birch KP, Downs MJ. Correction to the updated Edlén equation for the refractive index of air. Metrologia 1994;31(4):315–6.
[14] Ciddor PE. Refractive index of air: new equations for the visible and near infrared. Appl Opt 1996;35(9):1566–73.
[15] Blackburn C, Sawyer D, Shakarji C. Common-path method for laser tracker ranging calibration. J CMSC 2014;9(1):4–7.
[16] Stone JA, Decker JE, Gill P, Juncar P, Lewis A, Rovera GD, et al. Advice from the CCL on the use of unstabilized lasers as standards of wavelength: the helium–neon laser at 633 nm. Metrologia 2009;46(1):11–8.
[17] Quinn TJ. Practical realization of the definition of the metre, including recommended radiations of other optical frequency standards (2001). Metrologia 2003;40:103–33.
[18] Froome KD, Bradsell RH. Distance measurement by means of a light ray modulated at a microwave frequency. J Sci Instrum 1961;38:458–62.
[19] Thiel J, Pfeifer T, Hartmann M. Interferometric measurement of absolute distances of up to 40 m. Measurement 1995;16(1):1–6.
[20] Payne JM, Parker D, Bradley RF. Rangefinder with fast multiple range capability. Rev Sci Instrum 1992;63(6):3311–6.
[21] Stone JA, Stejskal A, Howard L. Absolute interferometry with a 670-nm external cavity diode laser. Appl Opt 1999;38(28):5981–94.
[22] Tilford CR. Analytical procedure for determining lengths from fractional fringes. Appl Opt 1977;16(7):1857–60.
[23] Deumlich F. Surveying instruments. Berlin, New York: DeGruyter; 1982.
[24] Mooring BW. Calibration of a laser projection system. In: ASME Winter Annual Meeting, DSC, Vol. 29, Applications of Modeling and Identification to Improve Machine Performance. 1991. p. 33–41.
[25] Zhuang H, Roth ZS. Modeling gimbal axis misalignments and mirror center offset in a single-beam laser tracking measurement system. Int J Rob Res 1995;14(3):211–24.
[26] Loser R, Kyle S. Alignment and field check procedures for the Leica Laser Tracker LTD 500. In: Boeing Large Scale Optical Metrology Seminar. 1999.
[27] Muralikrishnan B, Sawyer D, Blackburn C, Phillips S, Borchardt B, Estler WT. ASME B89.4.19 performance evaluation tests and geometric misalignments in laser trackers. J Res Natl Inst Stand Technol 2009;114(1):21–35.
[28] Lin PD, Lu C-H. Modeling and sensitivity analysis of laser tracking systems by skew-ray tracing method. J Manuf Sci Eng 2005;127(3):654–62.
[29] Conte J, Santolaria J, Majarena AC, Brau A, Aguilar JJ. Identification and kinematic calculation of laser tracker errors. Procedia Eng 2013;63: 379–87.
[30] Ouyang JF, Liu WL, Sun DX, Yan YG. Laser tracker calibration using coordinate measuring machine. In: Proceedings of the ASPE 20th Annual Meeting. 2005.
[31] Gassner G, Ruland R. Laser tracker calibration – testing the angle measurement system, SLAC-PUB-13476; 2008.

[32] Martin D, Chetwynd DG. High precision angle calibration of robotic total stations and laser trackers. In: Proceedings of the SPIE, Vol. 7133. 2009.
[33] Giniotis V, Bručas D, Šiaudinytė L. Arrangement for vertical angle calibration of geodetic instruments. Mechanika 2009;5(79):59–62.
[34] Muralikrishnan B, Blackburn C, Sawyer D, Phillips S, Bridges R. Measuring scale errors in a laser tracker's horizontal angle encoder through simple length measurement and two-face system tests. J Res Natl Inst Stand Technol 2010;115(5):291–301.
[35] Lewis A, Hughes B, Forbes A, Sun W, Veal D, Nasr K. Determination of misalignment and angular scale errors of a laser tracker using a new geometric model and a multi-target network approach. In: MacroScale 2011 Recent Developments in Traceable Dimensional Measurements. 2011.
[36] Nasr KM, Hughes B, Forbes A, Lewis A. Determination of laser tracker angle encoder errors. EPJ Web Conf 2014;77:00002.
[37] Hughes B, Forbes A, Lewis A, Sun W, Veal D, Nasr K. Laser tracker error determination using a network measurement. Meas Sci Technol 2011; 22(4.).
[38] Steffey K. Understanding laser tracker targets. J CMSC 2010;5(2):4–11.
[39] Fuss B, Bell B, Bowden G, Ruland R. The SLAC design and manufacturing process of sphere-mounted reflectors. In: Proceedings of the 5th International Workshop on Accelerator Alignment. 1997.
[40] ASME B89.4.19-2006. Performance evaluation of laser-based spherical coordinate measurement systems; 2006.
[41] Yan Y, Wang Z, Huang J, Zhang M. Geometric error analysis for spherical mounted retroreflector in laser tracker. In: International Conference on Intelligent Computation Technology and Automation. 2010. p. 391–4.
[42] Takatsuji T, Goto M, Osawa S, Yin R, Kurosawa T. Whole-viewing-angle cat's-eye retroreflector as a target of laser trackers. Meas Sci Technol 1999;10(7):N87–90.
[43] Ouyang J, Liu W, Qu X, Yan Y. The effect of beam incident angles on cube corner retro-reflector measuring accuracy. In: Proceedings of the SPIE, Vol. 6834. 2007.
[44] Lau K, Yang Y, Liu Y, Song H. Dynamic performance evaluation of 6D laser tracker sensor. In: Performance Metrics for Intelligent Systems, PerMIS'10. 2010. p. 285–9.
[45] Snyder JJ. Paraxial ray analysis of a cat's-eye retroreflector. Appl Opt 1975;14(8):1825–8.
[46] Nakamura O, Goto M, Toyoda K, Takai N, Kurosawa T, Nakamata T. A laser tracking robot-performance calibration system using ball-seated bearing mechanisms and a spherically shaped cat's-eye retroreflector. Rev Sci Instrum 1994;65(4):1006–11.
[47] Zürcher W, Loser R, Kyle SA. Improved reflector for interferometric tracking in three dimensions. Opt Eng 1995;34(9):2740–3.
[48] Yang B, Friedsam H. Ray-tracing studies for a whole-viewing-angle retroreflector. In: Proceedings of the 6th International Workshop on Accelerator Alignment. 1999.
[49] Lin Y, Zhang G, Li Z. An improved cat's-eye retroreflector used in a laser tracking interferometer system. Meas Sci Technol 2003;14(6):N36–40.
[50] Chen X, Zhang GX, Zhao SZ, Duan FJ. Analysis and measurement for the optical error of the cat's eye retro-reflector. J Phys: Conf Series 2006;48:64–8.
[51] Liu W, Ouyang J, Qu X, Yan Y. Misalignment error calibration of faro retro probe for laser tracker system. Chin Opt Lett 2007;5(5):281–3.
[52] Parker DH. Multidirectional retroreflector assembly with a common virtual reflection point using four-mirror retroreflectors. Precis Eng 2005;29(3):361–6.
[53] Kyle S. Alternatives in 6DOF probing – more flexibility, lower cost, universal? Proceedings of the 21st Annual Coordinate Metrology Systems Conference. 2005.
[54] Gordon JA, Novotny DR, Curtin AE. A single pixel touchless laser tracker probe. In: Proceedings of the 31st Annual Coordinate Metrology Systems Conference. 2015.
[55] Kyle S. Optically jointed probing systems for large-volume coordinate metrology. J CMSC 2007;2(1.).
[56] Kyle S. Roll angle in 6DOF tracking. In: Proceedings of the 24th Annual Coordinate Metrology Systems Conference. 2008.
[57] Calkins JM, Salerno RJ. A practical method for evaluating measurement system uncertainty. In: Boeing Large Scale Optical Metrology Seminar. 2000.
[58] Sandwith S, Predmore R. Real-time 5-micron uncertainty with laser tracking interferometer systems using weighted trilateration. In: Boeing Large Scale Optical Metrology Seminar. 2001.
[59] Liu W, Wang Z. Coordinate uncertainty analyses of coupled multiple measurement systems. Meas Sci Technol 2010;21(6).
[60] Mitchell J, Spence A, Hoang M, Free A. Sensor fusion of laser trackers for use in large-scale precision metrology. In: Proceedings of the SPIE, Vol. 5263. 2004.
[61] Meid A, Sandwith S. Dynamic weighting of laser tracker measurements for bundle adjustment. In: Boeing Large Scale Optical Metrology Seminar. 2000.
[62] Predmore CR. Bundle adjustment of multi-position measurements using the Mahalanobis distance. Precis Eng 2010;34(1):113–23.
[63] Nakamura O, Goto M, Toyoda K, Tanimura Y, Kurosawa T. Development of a coordinate measuring system with tracking laser interferometers. CIRP Ann – Manuf Technol 1991;40(1):523–6.
[64] Nakamura O, Goto M. Laser interferometric calibration of microscan mechanisms by using three laser beams. Precis Eng 1993;15(1):39–43.
[65] Nakamura O, Goto M. Four-beam laser interferometry for three-dimensional microscopic coordinate measurement. Appl Opt 1994;33(1):31–6.
[66] Takatsuji T, Goto M, Kurosawa T, Tanimura Y, Koseki Y. The first measurement of a three-dimensional coordinate by use of a laser tracking interferometer system based on trilateration. Meas Sci Technol 1998;9(1):38–41.
[67] Takatsuji T, Koseki Y, Goto M, Kurosawa T. Restriction on the arrangement of laser trackers in laser trilateration. Meas Sci Technol 1998;9(8):1357–9.
[68] Takatsuji T, Koseki Y, Goto M, Kurosawa T, Tanimura Y. Laser tracking interferometer system based on trilateration and a restriction for the position of its laser trackers. In: Proceedings of the SPIE, Vol. 3479. 1998.
[69] Takatsuji T, Goto M, Kirita A, Kurosawa T, Tanimura Y. The relationship between the measurement error and the arrangement of laser trackers in laser trilateration. Meas Sci Technol 2000;11(5):477–83.
[70] Zhang GX, Li XH, Lin YB, Liu SG, Liu XL, Li XF, et al. A study on the optimal design of laser-based multi-lateration systems. CIRP Ann – Manuf Technol 2003;52(1):427–30.
[71] Langley RB. Dilution of precision. GPS World; 1999. p. 52–9.
[72] Zhuang H, Li B, Roth Z, Xie X. Self-calibration and mirror center offset elimination of a multi-beam laser tracking system. Rob Auton Syst 1992;9(4): 255–69.
[73] Lin Y, Zhang G. The optimal arrangement of four laser tracking interferometers in 3D coordinate measuring system based on multi-lateration. In: The International Symposium on Virtual Environments, Human-Computer Interfaces, and Measurement Systems, VECIMS 2003. 2003.
[74] Zhang D, Rolt S, Maropoulos PG. Modelling and optimization of novel laser multilateration schemes for high-precision applications. Meas Sci Technol 2005;16(12):2541–7.
[75] Nguyen TT, Amthor A, Ament C. Algorithm for a high precision contactless measurement system. ACTA IMEKO 2013;2(2):3–12.
[76] Zhuang H, Motaghedi SH, Roth ZS, Bai Y. Calibration of multi-beam laser tracking systems. Robot Comput Integr Manuf 2003;19(4):301–14.
[77] Schwenke H, Franke M, Hannaford J. Error mapping of CMMs and machine tools by a single tracking interferometer. CIRP Ann – Manuf Technol 2005;54(1):475–8.
[78] Muralikrishnan B, Lee V, Blackburn C, Sawyer D, Phillips S, Ren W, et al. Assessing ranging errors as a function of azimuth in laser trackers and tracers. Meas Sci Technol 2013;24(6.).
[79] Osawa S, Takatsuji T, Hong J, Noguchi H, Kurosawa T. Evaluation of the performance of a novel laser tracker used for coordinate measurements. In: Proceedings of the SPIE, Vol. 4401. 2001.
[80] Greeff GP. Multilateration laser tracker systems. In: Test and Measurement Conference. 2010. p. 31–41.
[81] Wendt K, Schwenke H, Wäldele F, Krawczyk M, Kniel K. Error mapping of large CMMs by sequential multi-lateration using a laser tracker. In: Proceedings of the 2nd EUSPEN International Conference. 2001.
[82] Umetsu K, Furutnani R, Osawa S, Takatsuji T, Kurosawa T. Geometric calibration of a coordinate measuring machine using a laser tracking system. Meas Sci Technol 2005;16(12):2466–72.
[83] Schwenke H, Schmitt R, Jatzkowski P, Warmann C. On-the-fly calibration of linear and rotary axes of machine tools and CMMs using a tracking interferometer. CIRP Ann – Manuf Technol 2009;58(1):477–80.
[84] Wendt K, Franke M, Härtig F. Measuring large 3D structures using four portable tracking laser interferometers. Measurement 2012;45(10):2339–45.
[85] Takeuchi K, Ibaraki S, Yano T, Takatsuji T, Osawa S, Sato O. Estimation of three-dimensional volumetric errors of numerically controlled machine tools by a laser tracker. In: Proc. of 14th International Conference on Mechatronics Technology (ICMT2010). 2010. p. 323–7.
[86] Wang J, Guo J, Zhang G, Guo B, Wang H. The technical method of geometric error measurement for multi-axis NC machine tool by laser tracker. Meas Sci Technol 2012;23(4.).
[87] Aguado S, Samper D, Santolaria J, Aguilar JJ. Laser tracker based volumetric verification of machine tools. Adv Mater Res 2012;498:151–6.
[88] Linares J-M, Chaves-Jacob J, Schwenke H, Longstaff A, Fletcher S, Flore J, et al. Impact of measurement procedure when error mapping and compensating a small CNC machine using a multilateration laser interferometer. Precis Eng 2014;38(3):578–88.
[89] Santolaria J, Majarena AC, Samper D, Brau A, Velázquez J. Articulated arm coordinate measuring machine calibration by laser tracker multilateration. Sci World J 2014. Article ID 681853.
[90] Ruland RE. The chesapeake laser tracker in industrial metrology. In: XX International FIG Congress. 1994.
[91] Caskey GW, Fronczek Jr CJ, Phillips SD. Laser trackers: traceability, uncertainty, and standardization – a report to the CMSC. NISTIR 6061; 1997.
[92] Clarke TA, Wang X, Forbes AB, Cross NR. The case for a consistent method of verifying the performance of large volume metrology systems. In: Proceedings of the 16th Annual Coordinate Metrology Systems Conference. 2000.
[93] Clarke TA, Wang X, Cross NR, Forbes AB, Fossati PM. Performance verification for large volume metrology systems. In: 5th International Conference on Laser Metrology and Machine Performance, LAMDAMAP. 2001. p. 105–16.
[94] Sawyer D, Borchardt B, Phillips S, Fronczek C, Estler T, Woo W, et al. A laser tracker calibration system. In: Measurement Science Conference. 2002.
[95] VDI/VDE 2617 Part 10: Accuracy of coordinate measuring machines – characteristics and their checking – acceptance and reverification tests of laser trackers.
[96] Draft ISO/DIS 10360-10: Geometrical product specifications (GPS)—acceptance and reverification tests for coordinate measuring systems (CMS): Part 10. Laser trackers for measuring point-to-point distances.

[97] Estler WT, Sawyer DS, Borchardt B, Phillips SD. Large-scale metrology instrument performance evaluations at NIST. J CMSC 2006;1(2):27–32.
[98] Muralikrishnan B, Sawyer D, Blackburn C, Phillips S, Borchardt B, Estler WT. Performance evaluation of laser trackers. In: Performance Metrics for Intelligent Systems, PerMIS'08. 2008.
[99] Ma L, Wang L, Cao T, Wang J, He X, Xiong C. A large-scale laser plane calibration system. Meas Sci Technol 2007;18(6):1768–72.
[100] Nasr K, Forbes A, Hughes B, Lewis A. ASME B89.4.19 standard for laser tracker verification – experiences and optimisations. Int J Metrol Qual Eng 2012;3(2):89–95.
[101] Muralikrishnan B, Sawyer D, Blackburn C, Phillips S, Shakarji C, Morse E, et al. Choosing test positions for laser tracker evaluation and future standards development. J CMSC 2011;6(1):12–9.
[102] Bryan JB. A simple method for testing measuring machines and machine tools Part 1: principles and applications. Precis Eng 1982;4(2):61–9.
[103] Knapp W, Tschudi U, Bucher A. Comparison of different artefacts for interim coordinate-measuring machine checking: a report from the Swiss standards committee. Precis Eng 1991;13(4):277–91.
[104] Phillips SD, Borchardt B, Doiron T, Henry J. Properties of free-standing ball bar systems. Precis Eng 1993;15(1):16–24.
[105] Cauchick-Miguel P, King T, Davis J. CMM verification: a survey. Measurement 1996;17(1):1–16.
[106] Ziegert J, Rea D, Phillips SD, Borchardt B, Stoup J. Design and testing of a one dimensional measuring machine for determining the length of ball bars. In: Proceedings of the ASPE 16th Annual Meeting. 2001.
[107] Phillips S, Sawyer D, Borchardt B, Ward D, Beutel D. A novel artifact for testing large coordinate measuring machines. Precis Eng 2001;25(1):29–34.
[108] Sawyer D, Parry B, Phillips S, Blackburn C, Muralikrishnan B. A model for geometry-dependent errors in length artifacts. J Res Natl Inst Stand Technol 2012;117:216–30.
[109] Hudlemeyer A, Meuret M, Sawyer D, Blackburn C, Lee V, Shakarji C. Consideration for design and in-situ calibration of high-accuracy length artifacts for field testing of laser trackers. J CMSC 2015;10(1):26–32.
[110] Lee VD, Blackburn C, Muralikrishnan B, Sawyer D, Meuret M, Hudlemeyer A. A proposed interim check for field testing a laser tracker's 3D length measurement capability using a calibrated scale bar as a reference artifact. NISTIR 8016; 2014.
[111] JCGM 200:2008. International vocabulary of metrology – basic and general concepts and associated terms (VIM). 3rd ed; 2008.
[112] ASME B89.7.5-2006. Metrological traceability of dimensional measurements to the SI unit of length; 2006.
[113] Swyt DA, Phillips SD, Palmateer J. Developments at NIST on traceability in dimensional measurements. In: Proceedings of the SPIE, Vol. 4401. 2001. p. 245–52.
[114] Phillips S, Krystek M, Shakarji C, Summerhays K. Dimensional measurement traceability of 3D imaging data. In: Proceedings of the SPIE, Vol. 7239. 2009.
[115] Morse E, Welty V. Dynamic testing of laser trackers. CIRP Ann – Manuf Technol 2015;64(1):475–8.
[116] Liu WL, Wang Z, Wang S, Li X. Error correction for laser tracking system using dynamic weighting model. Adv Mech Eng 2013;5.
[117] Sandwith S. Thermal stability of laser tracking interferometer calibration. In: Proceedings of the SPIE, Vol. 3835. 1999.
[118] Ouyang J, Liang Z, Zhang H, Yan Y. Research of measuring accuracy of laser tracker system. In: Proceedings of the SPIE, Vol. 6280. 2006.
[119] JCGM 100:2008. Evaluation of measurement data—guide to the expression of uncertainty in measurement. 1st ed; 2008.
[120] Li J, Wu S, Wu F, Kuang L, Cao X. Evaluate the task-specific measurement uncertainty of laser tracker using Monte-Carlo method. In: Proceedings of the SPIE, Vol. 7656. 2010.
[121] Wang J, Guo J, Wang H, Deng Y. The evaluation of measurement uncertainty for laser tracker based on Monte Carlo method. In: Proceedings of the 2011 IEEE International Conference on Mechatronics and Automation. 2011. p. 608–12.
[122] Yang J, Li G, Wu B, Gong J, Wang J. Comparison of GUF and Monte Carlo methods to evaluate task-specific uncertainty in laser tracker measurement. J Cent South Univ 2014;21(10):3793–804.
[123] Baldwin JM, Summerhays KD, Campbell DA, Henke RP. Application of simulation software to coordinate measurement uncertainty evaluations. Measure 2007;2(4):40–52.
[124] Forbes A. Surface fitting taking into account uncertainty structure in coordinate data. Meas Sci Technol 2006;17(3):553–8.
[125] Forbes AB. Uncertainty evaluation associated with fitting geometric surfaces to coordinate data. Metrologia 2006;43(4):S282–90.
[126] Forbes AB, Hughes B, Sun W. Comparison of measurements in co-ordinate metrology. Measurement 2009;42(10):1473–7.
[127] Huo D, Maropoulos PG, Cheng CH. The framework of the virtual laser tracker – a systematic approach to the assessment of error sources and uncertainty in laser tracker measurement. In: Proceedings of the 6th CIRP-Sponsored International Conference on Digital Enterprise Technology. 2010. p. 507–23.
[128] Peggs G. Virtual technologies for advanced manufacturing and metrology. Int J Comput Integr Manuf 2003;16(7–8):485–90.
[129] Forbes AB. Efficient algorithms for structured self-calibration problems. In: Algorithms for Approximation IV, Proceedings of the 2001 International Symposium. 2001.
[130] Ulrich T. Uncertainty estimation and multi sensor fusion for kinematic laser tracker measurements. Metrologia 2013;50(4):307–17.
[131] Ulrich T, Irgenfried S. Uncertainty estimation for kinematic laser tracker measurements incorporating the control information of an industrial robot. In: 2014 International Conference on Indoor Positioning and Indoor Navigation. 2014.
[132] Martin J. Metrology automation is here and now. Qual Mag 2014.
[133] Kihlman H, Loser R, Cooke A, Sunnanbo A, Arb KV. Metrology-integrated industrial robots – calibration, implementation and testing. In: Proceedings of the 35th International Symposium on Robotics. 2004.
[134] Muelaner JE, Wang Z, Jamshidi J, Maropoulos PG. Verification of the indoor GPS system by comparison with points calibrated using a network of laser tracker measurements. In: Proceedings of the 6th CIRP-Sponsored International Conference on Digital Enterprise Technology. 2010. p. 607–19.
[135] Wang Z, Mastrogiacomo L, Franceschini F, Maropoulos P. Experimental comparison of dynamic tracking performance of iGPS and laser tracker. Int J Adv Manuf Technol 2011;56(1–4):205–13.
[136] Eger JS, Porath M, Donatelli GD. Sequential multilateration technique for the determination of 3D coordinates of reference points in industrial geodesy using a high-accuracy self-tracking laser interferometer. In: Proceedings of the 11th International Symposium on Measurement Technology and Intelligent Instruments. 2013.
[137] MacKinnon DK, Cournoyer L, Beraldin J-A. Single-plane versus three-plane methods for relative range error evaluation of medium-range 3D imaging systems. In: Proceedings of the SPIE, Vol. 9528. 2015.
[138] Ferrucci M, Muralikrishnan B, Sawyer D, Phillips S, Petrov P, Yakovlev Y, et al. Evaluation of a laser scanner for large volume coordinate metrology: a comparison of results before and after factory calibration. Meas Sci Technol 2014;25(10):25.
[139] Saadat M, Cretin L. Measurement systems for large aerospace components. Sens Rev 2002;22(3):199–206.
[140] Muelaner J, Maropoulos P. Large scale metrology in aerospace assembly. In: Proceedings of the 5th International Conference on Digital Enterprise Technology. 2008.
[141] Sabino A. Aerospace pushes manufacturing to new heights with laser trackers. Qual Dig 2009.
[142] Williams G, Chalupa E, Rahhal S. Automated positioning and alignment systems. SAE Tech Pap 2000-01-3014; 2000.
[143] Rakich A. Alignment of LBT optics using a laser tracker. In: Proceedings of the SPIE, Vol. 7733. 2010.
[144] Burge JH, Su P, Zhao C, Zobrist T. Use of a commercial laser tracker for optical alignment. In: Proceedings of the SPIE, Vol. 6676. 2007.
[145] Zobrist TL, Burge JH, Martin HM. Laser tracker surface measurements of the 8.4 m GMT primary mirror segment. In: Proceedings of the SPIE, Vol. 7426. 2009.
[146] Bryce EA, Gallegos FH. Compact-range coordinate system established using a laser tracker. Sandia Rep SAND2006-7541; 2006.
[147] Juretzko M, Richter E. Geometrical survey of compact antenna test ranges using laser tracker technology. In: 3rd IAG/12th FIG Symposium. 2006.
[148] Martin D. Review of accelerator alignment. In: FIG Congress 2010, Facing the Challenges – Building the Capacity. 2010.
[149] Wojcik GJ, Lakanen SA. Laser tracker, a handy tool for metrology and alignment. In: Proceedings of the 7th International Workshop on Accelerator Alignment. 2002.
[150] Kalantar DH, Di Nicola P, Shingleton N, Burkhart S, Dzenitis J, Klingmann J, et al. An overview of target and diagnostic alignment at the National Ignition Facility. In: Proceedings of the SPIE, Vol. 8505. 2012.